

## NANOTRIBOLOGY

**Enrico Gnecco**

*Department of Physics. University of Basel, Switzerland*

**Keywords:** Atomic stick-slip, Friction force microscopy, Load dependence of friction, Nanocontacts, Nanoindentation, Nanolithography, Nanowear, Superlubricity, Tomlinson model, Velocity dependence of friction.

### Contents

1. Introduction
  2. Instruments
  3. Mechanics of sliding nanocontacts
  4. Friction experiments on the nanometer scale
  5. Modeling friction on the atomic scale
  6. Friction experiments on the atomic scale
  7. Wear on the nanometer scale
  8. Conclusions
- Glossary  
Bibliography  
Biographical Sketch

### Summary

In the last 20 years, experiments performed with the atomic force microscope gave new insight into the physics of single asperities sliding over solid surfaces. These results, together with complementary experiments realized by surface force apparatus and quartz microbalance, established the field of nanotribology. At the same time, increasing computing power allowed for the simulation of mechanical processes in sliding contacts consisting of several hundred atoms. Atomic processes cannot be neglected in the interpretation of nanotribology experiments. Experiments on well-defined surfaces reveal indeed atomic structures in friction forces. The chapter begins with an introduction on friction force microscopy, including the calibration of cantilever force sensors. After an overview of contact models and experiments on the nanometer scale, we introduce the Tomlinson model, which is commonly used to interpret atomic stick-slip. Measurements of friction on the atomic scale are discussed, which revealed important effects like superlubricity and thermal activation. The onset of wear on atomic scale has recently come into the scope of experimental studies and is described in the last chapter. Important topics like dissipation in non-contact force microscopy and electronic friction are also mentioned.

### 1. Introduction

The term *tribology* (from the Greek word *tribos* = *to rub*) refers to the study of friction, wear, lubrication and contact mechanics. Significant parts of gross domestic product of industrialized countries are wasted every year because of tribological problems, which

originate from complex processes occurring on the nanometer scale. These processes are extremely important in data storage and microelectronics industry. In order to achieve high recording densities in magnetic storage devices the height of the read/write magnetic head with respect to the magnetic medium has to be reduced. This may lead to contact with serious consequences. In microelectromechanical systems, objects a few micrometers in size are repeatedly brought into contact at high speed. In both cases the resistance to rupture of different coatings and components needs to be tested and controlled on the small scale.

The macroscopic results of tribology cannot be simply scaled down to the micro and nano-world. If the linear size of a component is reduced by a factor of ten, the area of its surface decreases ten times less than its volume, which implies that the resistive forces, proportional to the area of sliding, decrease ten times less than the inertial forces, proportional to the volume of the component. The observation of tribological processes on the nanometer scale became possible with the introduction of the *atomic force microscope* (AFM). With this instrument the forces acting on a sharp tip sliding on a surface can be measured from the deformation of a micro cantilever supporting the tip (Figure 1). The normal force between tip and surface causes the vertical deflection of the cantilever, whereas the friction force causes its torsion. If the vertical deflection is kept constant by a feedback loop, friction can be monitored at a given load while scanning. In such a context, the AFM is also called *friction force microscope* (FFM). How to detect friction with AFM is the subject of Section 2. Other instruments of interest in nanotribology are the surface force apparatus and the quartz crystal microbalance. are also briefly described.

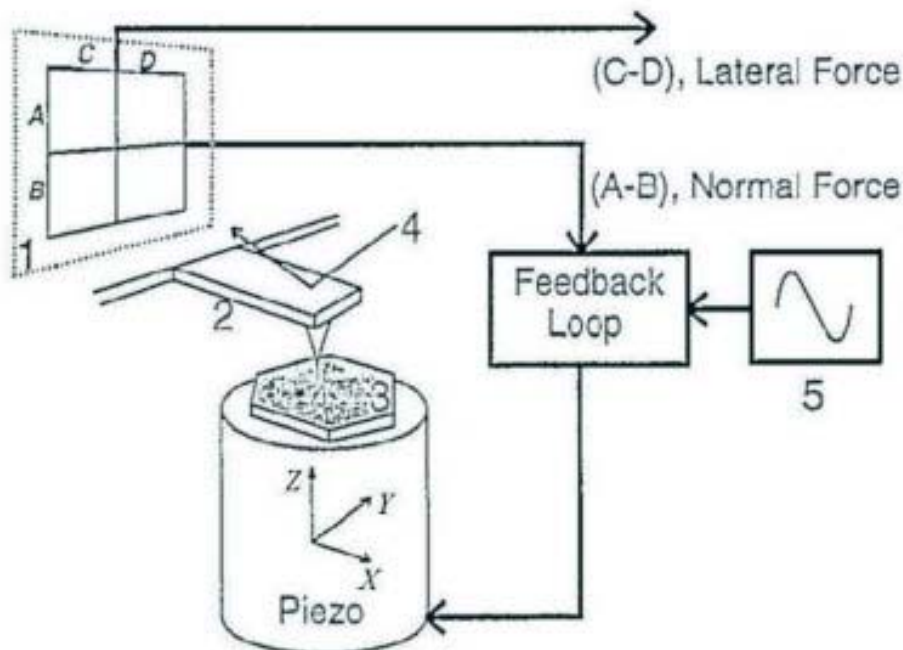


Figure 1. Sketch of a beam-deflection friction force microscope. (1) Four-quadrant photodiode; (2) Cantilever with integrated probing tip; (3) Segmented piezoelectric tube with sample; (4) Ray trace of the laser beam. Reprinted from R. Lüthi et al., *Surf. Sci.* 338, 247 (1995) © 1995 by Elsevier Science

The contact between two macroscopic surfaces is made by thousands of micro junctions. When the AFM tip slides on a flat surface a junction a few nanometers in size is formed. The mechanical response of a single asperity to sliding is quite different from the response of several asperities. If the tip has a spherical shape the friction or lateral force,  $F_L$ , is related to the normal force,  $F_N$ , by the *Hertzian relation*  $F_L \propto F_N^{2/3}$ . This relation is substantially different from the well-known *Amonton's law*,  $F_L \propto F_N$ . However, the Amonton's law is recovered once statistical distributions of single asperities are considered. Adhesion plays also an important role in the contact region, and is taken into account in extended Hertzian models. These models, which are in good agreement with FFM experiments, are discussed in Section 3.

In a well-defined environment, the friction force acting on a sliding asperity depends on the surface under investigation. Due to the small size of the tip (typical radii of curvature are 10-50 nm) the AFM can map friction forces on a local scale with extraordinary resolution. Several friction maps on the nanometer scale are discussed in Section 4. Friction maps with atomic features were first detected in 1987 on graphite. Figure 2a shows a friction map of sodium chloride acquired in ultra-high vacuum (UHV). The structure of the atomic lattice is well reproduced. A single scan line presents a saw-tooth shape, as shown in Figure 2b. When the scan direction is inverted the friction force is also inverted. The area of the *friction loop* obtained after scanning forwards and backwards corresponds to the energy dissipated per scan cycle. The sawtooth shape is caused by the *stick-slip* motion of the AFM tip, which periodically jumps from a stable equilibrium position on the atomic lattice into the next one. A simple explanation of the atomic stick-slip is given by the *Tomlinson model*, which is discussed in Section 5. If thermal effects are included, the Tomlinson model predicts a logarithmic dependence of friction on the scan speed. This in contrast with the classical *Coulomb's law* of friction, which states that friction is speed-independent. Section 6 deals with friction measurements on the atomic scale and related phenomena, such as friction anisotropy, dissipative effects in close contact with the sample surface, and electronic friction.

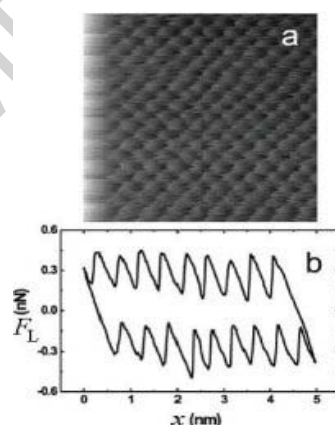


Figure 2. (a) Friction map acquired on a NaCl(100) surface (forward scan direction). (b) Friction loop taken across Figure 2a and corresponding back scan image. Reprinted from E.Gnecco et al., *Phys. Rev. Lett.* 84, 1172 (2000). © 2000 by the American Physical Society

If the normal load applied on the AFM tip overcomes a critical value, the morphology of the surface is permanently damaged. In exceptional cases wear processes can be studied down to the atomic scale. Tip-induced modifications of surfaces on the nanoscale are discussed in Section 7.

## 2. Instruments

### 2.1. Friction Force Microscopy

The basic principle of AFM is sketched in Figure 1. A scanner formed by piezoelectric elements moves a sharp tip relatively to a flat surface sample with a certain periodicity. The scanner can be also extended or retracted to vary the normal force,  $F_N$ , between tip and surface. This force causes the vertical deflection of the cantilever supporting the tip. If the normal force increases while scanning, due to the local slope of the surface, the scanner is retracted by a feedback loop to keep the force  $F_N$  constant. On the other hand, if  $F_N$  decreases, the surface is brought closer to the tip by extending the scanner. In such a way, the topography of the surface can be determined line by line. An accurate control of the piezo movement is made possible by a laser beam, which is reflected from the rear of the cantilever into a photodetector. When the bending of the cantilever changes, the laser spot on the detector moves up or down. The difference signal between upper and lower segments of the photodiode (A-B) is proportional to the normal force  $F_N$ .

The relative sliding of tip and surface is also accompanied by *friction*. A lateral force,  $F_L$ , with the opposite direction of the scan velocity, hinders the motion of the tip. The force  $F_L$  causes the torsion of the cantilever and it can be observed with the topography if the photodetector can reveal not only the vertical deflection, but also the lateral movement of the cantilever while scanning. In practice, this is realized by four-quadrants photodetectors, where the difference signal between left and right segments (C-D) is proportional to the lateral force  $F_L$ . Incidentally, friction causes also the lateral bending of the cantilever, but this effect is negligible if the thickness of the cantilever is much smaller than its width.

Besides optical beam deflection the forces between tip and surface can also be measured by capacitance detection, dual fiber interferometry, and piezolevers. In the first method, two plates close to the cantilever reveal capacitance variations while scanning. The second technique uses two optical fibers to detect the cantilever deflection along two orthogonal directions angled  $45^\circ$  with the respect to the surface normal. In the third method, cantilevers with two Wheatstone bridges at their base are used. Normal and lateral forces are respectively proportional to the sum and the difference of both bridge signals.

## 2.2. Force Calibration in Friction Force Microscopy

Force calibration is relatively simple when rectangular cantilevers are used. Due to possible discrepancies with the values provided by manufacturers, optical and electron microscopes should be used to determine the width  $w$ , the thickness  $t$  and the length  $l$  of the lever, as well as the tip height,  $h$ , and the position of the tip with respect to the cantilever. The cantilever thickness can also be inferred from the resonance frequency,  $f_0$ , using the relation:

$$t = \frac{2\sqrt{12}\pi}{1.875^2} \sqrt{\frac{\rho}{E}} f_0 l^2. \quad (1)$$

In (1)  $\rho$  is the cantilever density, and  $E$  is its Young's modulus. The normal spring constant,  $c_N$ , and the lateral spring constant,  $c_L$ , are given by

$$c_N = \frac{Ewt^3}{4l^3}, \quad c_L = \frac{Gwt^3}{3h^2l}, \quad (2)$$

where  $G$  is the shear modulus of the cantilever. The next step consists in measuring the sensitivity of the photodetector,  $S_z$  (nm/V). The sensitivity of a beam-deflection AFM can be obtained by force vs. distance curves on hard surfaces, where elastic deformations are negligible and the vertical movement of the scanner equals the cantilever deflection. A typical relation between the difference of the vertical signals on the four-quadrant detector,  $V_{A-B}$ , and the distance from the surface,  $z$ , is sketched in Figure 3. When the tip is approached no signal is revealed until the tip jumps into contact at  $z = z_1$ . Further extension or retraction of the scanner result in a linear response until the tip jumps again out of contact at a distance  $z_2 > z_1$ , due to adhesive forces. The slope of the linear part of the curve gives the required sensitivity,  $S_z$ . Assuming that the laser beam is well positioned above the probing tip, the normal and lateral forces are related to the voltage  $V_{A-B}$ , and the difference between the horizontal signals,  $V_{C-D}$ , on the photodetector by the following relations:

$$F_N = c_N S_z V_{A-B}, \quad F_L = \frac{3}{2} c_L \frac{h}{l} S_z V_{C-D} \quad (3)$$

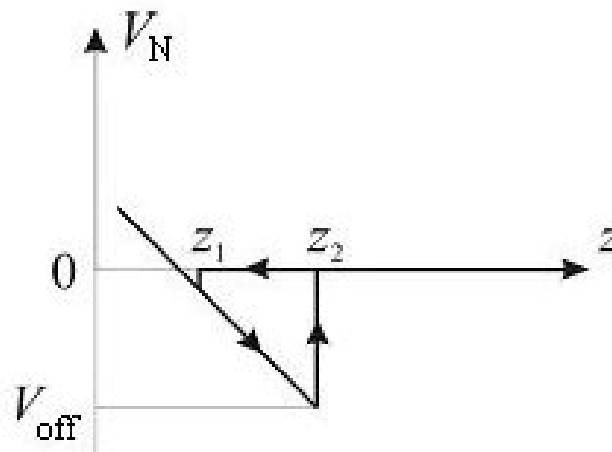


Figure 3. Sketch of a typical force vs. distance curve. The tip approaches the sample from right to left. At  $z = z_1$  the tip jumps into contact. Further motion results in elastic bending of the cantilever. The tip jumps out of contact at  $z_2 > z_1$ .

The normal spring constant  $c_N$  can also be evaluated with other methods. If little spheres are attached to the tip, the resonance frequency  $f_0$  changes according to the formula

$$f_0 = \frac{1}{2\pi} \sqrt{\frac{c_N}{M + m^*}}. \quad (4)$$

In (4)  $M$  is the mass of the added object and  $m^*$  is a certain effective mass of the cantilever, which depends on its geometry. The spring constant can thus be estimated from the frequency shifts corresponding to the different masses attached. The constant  $c_N$  is also related to the area of the power spectrum of the thermal fluctuations of the cantilever,  $P$ . The correct relation is  $c_N = 4k_B T / 3P$ , where  $k_B = 1.38 \times 10^{-3}$  J/K is the Boltzmann constant and  $T$  is the temperature. Cantilevers with different shape require finite element analysis, although in few cases (for instance V-shaped cantilevers) approximated analytical formulas can be derived. Surfaces with well-defined profiles may also be used as *in situ* tools for calibration. In such a case the horizontal and vertical components of the total force revealed by the photodetector differ from the normal and lateral components with respect to the surface,  $F_N$  and  $F_L$ . The geometric relations between these components determine the conversion ratio between volts and nanonewtons.

In some cases an adequate estimation of the radius of curvature of the tip,  $R$ , is also required. This quantity can be measured using a scanning electron microscope. Otherwise, well-defined structures as step sites or whiskers can be imaged. The image of these high-aspect ratio structures is convoluted with the tip shape. Deconvolution algorithms allow us to extract the radius of curvature of the probing tip.

Finally, when calibrating the FFM one must be aware that the accuracy of the piezoelectric scanners is limited by instrumental drifts and typical piezoelectric effects such as non-linearity, hysteresis, creep and variation of sensitivity with the applied voltage may become relevant.

### 2.3. Other Techniques

Besides the atomic force microscope, other important instruments in nanotribology are the *surface force apparatus* (SFA) and the *quartz crystal microbalance* (QCM).

The SFA consists of a pair of mica sheets, which are pressed together and reciprocally translated under pressure. The contact area and distance between mica surfaces can be measured by optical or capacitive techniques with resolution of 2 Å. The normal and lateral forces are determined from the deformation of springs. The SFA is commonly used to detect the behavior of lubricant liquids between the two surfaces in contact. For instance, the ordering of liquids in discrete layers has been observed as a function of the applied load. This effect could also be revealed an AFM. In such a case, the layering of liquid molecules on the surfaces caused stiffness oscillation as the tip-sample distance was varied.

The QCM consists of a single crystal of quartz, which oscillates in a shear mode with a high quality factor  $Q$ . If a thin film slides on the crystal surface, frequency shift and broadening of the resonance peak is observed. Unfortunately, the QCM can reveal only very low friction forces and its application is limited to systems like rare-gas solids on metals. In Section 6.5 we will see how this instrument has been used to detect electronic contributions to friction.

-  
-  
-

TO ACCESS ALL THE 30 PAGES OF THIS CHAPTER,  
Visit: <http://www.eolss.net/Eolss-sampleAllChapter.aspx>

### Bibliography

Dienwiebel et al. (2004). Superlubricity of graphite. *Phys. Rev. Lett.* 92, 126101. [Onset of structural lubricity]

Gnecco E. et al. (2000). Velocity dependence of atomic friction. *Phys. Rev. Lett.* 84, 1172-1175. [Influence of thermal activation on atomic-scale friction maps]

Gnecco et al. (2002). Abrasive wear on the atomic scale. *Phys. Rev. Lett.* 88, 215501. [First FFM maps of scratched surfaces showing atomic-scale features]

Lüthi et al. (1994). Sled-type motion on the nanometer scale: Determination of dissipation and cohesive

energy of C<sub>60</sub>. *Science* 266, 1979-1981. [Measurements of friction between manipulated nano-islands and surfaces]

Mate C.M. et al. (1987). Atomic-scale friction of a tungsten tip on a graphite surface. *Phys. Rev. Lett.* 59, 1942-1945. [First FFM maps showing atomic-scale features]

Socoliuc A. et al. (2004). Transition from stick-slip to continuous sliding in atomic friction: Entering a new regime of ultralow friction. *Phys. Rev. Lett.* 92, 134301. [Superlubricity onset at ultralow loads]

Socoliuc A. et al. (2006). Atomic-scale control of friction by actuation of atomic-size contacts. *Science* 313, 207-210. [Superlubricity induced by exciting contact resonance frequencies]

Zykova-Timan et al. (2007). Peak effect versus skating in high temperature nanofriction. *Nat. Mat.* 6, 230. [Simulations of nanofriction close to the melting point of an ionic crystal]

### **Biographical Sketch**

**Enrico Gnecco** was born in Genova, Italy, in 1972. He was awarded a PhD in Physics from the University of his hometown, with a thesis on nanotribological properties of amorphous carbon films. Since 2000 he has been working at the University of Basel, Switzerland, where he investigated several properties of friction and wear on the nanoscale, including velocity dependence of friction, wear onset on ionic crystals, transition from stick-slip to superlubricity, and superlubric imaging. He also studied self-assembling of organic molecules on ionic crystals and has recently started to address controlled manipulation of nanoparticles by atomic force microscopy. He co-authored more than 40 peer-reviewed publications (including articles on *Science*, *Nanoletters*, and *Physical Review Letters*) and 4 book chapters. He also authored the book "Nanoscale Processes on Insulating Surfaces" (World Scientific, 2009) with Prof. M. Szymonski, and edited the book "Fundamentals of Friction and Wear on the Nanoscale" (Springer, 2007) with Prof. E. Meyer.